CONFERENCE PRE-PRINT

SIMULATION OF TUNGSTEN EROSION AND EDGE-TO-CORE TRANSPORT IN NEON-SEEDED JET PLASMAS

¹H.A. KUMPULAINEN, ²P. INNOCENTE, ¹S. BREZINSEK, ¹A. KIRSCHNER, ¹J. ROMAZANOV, ³C. GIROUD, ⁴D. FAJARDO, ¹A. HUBER, ³E. LITHERLAND-SMITH, ⁵E. PAWELEC, ¹G. SERGIENKO, ²N. VIANELLO, ⁶S. WIESEN, ³A. MEIGS, ³S. MENMUIR, ³A. BOBOC, ³D. KOS, ³Z. HUANG, JET CONTRIBUTORS* AND THE EUROFUSION TOKAMAK EXPLOITATION TEAM**

¹Forschungszentrum Jülich GmbH, Jülich, Germany

Email: h.kumpulainen@fz-juelich.de

Abstract

The capability of simulation tools to predict tungsten (W) erosion and transport in fusion edge and core plasmas is evaluated by studying JET ELM-free H-mode plasmas with neon seeding. The background plasma profiles are interpretatively modelled using SOLEDGE3X-EIRENE with cross-field drifts and SOLEDGE2D-EIRENE without cross-field drifts for the edge plasma and JINTRAC for the core. ERO2.0 simulations predict the W erosion rate and W transport in the edge plasma, establishing the boundary condition for the W density in JINTRAC core transport simulations. The predicted W erosion sources are validated by comparing synthetic and measured W I line emission in the low-field side (LFS) divertor. The predicted W density profile and radiated power density in the core plasma is validated against an integrated data analysis of core diagnostics. Code-experiment agreement is reached within a factor of 3 in the core plasma; the W density is overpredicted when cross-field drifts are neglected in the edge plasma background but underpredicted when the drifts are included. The level of agreement is within the modelling uncertainties induced by the accuracy of the simulated background plasma conditions and diagnostic coverage.

1. INTRODUCTION

Predicting the tungsten (W) density in fusion devices is a critical component in assessing the expected performance of ITER and other future devices employing a W first wall. In recent years, continued validation of W erosion and transport simulations at JET with the beryllium (Be)/W ITER-like wall has demonstrated agreement with experimentally inferred core plasma W densities in deuterium (D) L-mode and H-mode plasmas within the estimated modelling uncertainties, up to a factor of 2 for L-mode and a factor of 3 for H-mode [1, 2]. The presented contribution describes the first application of the predictive W erosion and transport simulation workflow to the JET-ITER baseline scenario [3] which involves several new crucial factors: neon (Ne) seeding, vertical-vertical divertor target configuration, and H-mode energy confinement without type-I edge-localised modes (ELMs). The JET-ITER baseline plasmas provide a unique dataset on core-pedestal-exhaust integration, which is the subject of extensive analysis and validation of edge and core modelling frameworks [4], including the presented work.

The focus of the study is JET D plasma discharge #97490 during the stationary time interval 13.7 to 15.2 seconds, with an axial magnetic field B_T = 2.7 T, plasma current I_p = 2.5 MA, auxiliary heating power P = 34 MW, core electron density n_e = $0.9 \cdot 10^{20}$ m⁻³ and ion temperature T_i = 7 keV, as well as Ne concentration 1.75% in the pedestal. The divertor configuration, triangularity, safety factor profile, D_2 fuelling, and Ne seeding rates are chosen for maximum similarity with ITER stationary core-edge-integrated power exhaust and confinement scaling within the operational constraints of JET.

²Consorzio RFX, Padova, Italy

³UKAEA, Culham Campus, Abingdon, UK

⁴Max-Planck-Institut für Plasmaphysik, Garching, Germany

⁵Institute of Physics, University of Opole, Opole, Poland

⁶DIFFER - Dutch Institute for Fundamental Energy Research, Eindhoven, Netherlands

^{*}See the author list of CF. Maggi et al., Nucl. Fusion 2024, 10.1088/1741-4326/ad3e16

^{**}See the author list of E. Joffrin Nuclear Fusion 2024 10.1088/1741-4326/ad2be4

2. METHODS

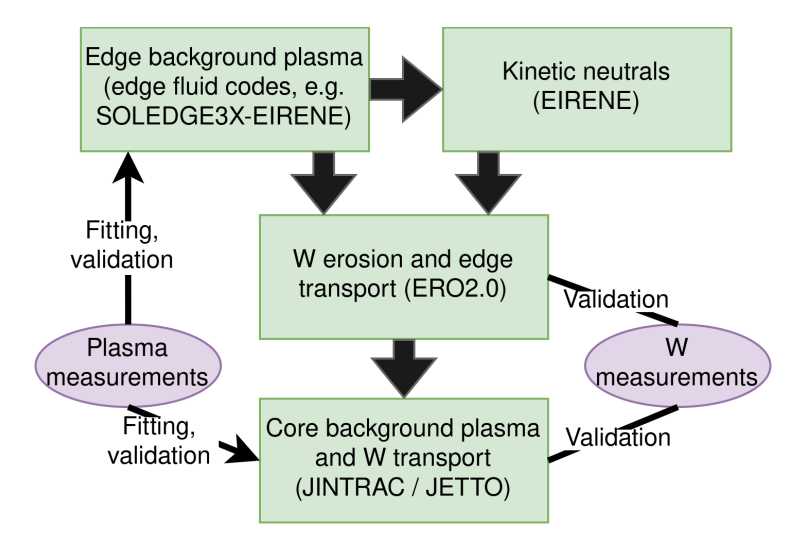


FIG. 1. Simulation and validation workflow for predictive W erosion and transport with interpretive background plasma profiles.

The applied methodology for predicting W erosion and transport is a multi-code workflow (Fig. 1) which involves high-fidelity physics models for each simulation stage and avoids the excessive computational cost and technical challenges associated with simulating all relevant processes in a single integrated simulation. While no information from W diagnostics is used as input, the simulated plasma conditions are iteratively adjusted to measurements, reducing the substantial uncertainty induced by the background plasma. The modelling approach couples the SOLEDGE3X-EIRENE [5] edge plasma fluid code with the EIRENE [6] kinetic neutral transport code to model the background plasma and the neon impurities in the edge plasma. The background plasma simulations are performed with (SOLEDGE3X) and without (SOLEDGE2D) the cross-field drifts. The toroidally symmetric 'wide-grid' computational domain extends from the core boundary (normalised minor radius $\rho = 0.87$) to the limiter contours. An additional stand-alone EIRENE simulation is set up for the converged SOLEDGE3X-EIRENE solution to record the spatially resolved bivariate energy-angular impact distribution [7] of atoms, particularly D charge-exchange neutrals (CXN), with an increased amount of particle histories (by a factor of 100).

The output from SOLEDGE3X and EIRENE simulations is used as input data for the ERO2.0 [8] 3D trace-impurity Monte Carlo code, which calculates the W erosion rate on plasma-facing surfaces due to each incident particle species, and follows the trajectories of the eroded W until deposition. Spatially resolved volumetric profiles of the electron density, electron and ion temperature, parallel-B and radial electric field, main ion parallel-B flow velocity, electron and ion conductive parallel-B heat flux, ion anomalous cross-field diffusivity, and density of each Ne charge state are extracted from the SOLEDGE3X solution to ERO2.0. In addition to the volumetric profiles, the flux and temperature of each ion species, as well as the flux and energy-angular distribution of incident atoms, are mapped onto the 3D plasma-facing surfaces. The intrinsic Be impurity flux to W surfaces is prescribed as a spatially constant 0.5% concentration in charge state Be²⁺. The sputtering yield database used by ERO2.0 includes physical but not chemical sputtering of W by the incident D, Be, Ne, and W projectiles.

Besides the input data from SOLEDGE3X and EIRENE, the toroidal rotation frequency profile and the spatially resolved neoclassical cross-field diffusive and convective transport coefficients are prescribed in ERO2.0. The rotation frequency is determined from charge-exchange recombination spectroscopy and the neoclassical transport coefficients are obtained from NEO [9] simulations.

The ERO2.0 simulation is repeated for several time steps until the W self-sputtering rate, calculated from the wall impacts of traced W trajectories, converges to a steady state. The orbit-tracing method adaptively changes between full-orbit resolution near wall surfaces (for prompt redeposition) and guiding-center

H.A. KUMPULAINEN et al.

approximation elsewhere. ERO2.0 calculates synthetic W I line emission intensities along designated lines of sight, used for experimental validation of the simulated W erosion rate. The flux-surface-averaged total W density predicted by ERO2.0 at the pedestal top (ρ = 0.9) is used as a boundary condition for core W transport simulations using JETTO [10], which is part of the JINTRAC [11] suite of codes.

The JETTO simulations describe the core plasma consisting of main ions and electrons as well as Ne, nickel (Ni), and W impurities. The surrogate model QuaLiKiz-NN [12] is used for turbulent transport, and combined with an additional contribution of Bohm-gyro-Bohm [13] transport which is adjusted by ad-hoc multipliers iteratively optimised to replicate the n_e , T_e , and T_i profiles. Neoclassical transport is accounted for using NEO for impurities and NCLASS [14] for the main ions. The heating, radiation, current, and rotation profiles and the fuelling rate are prescribed. The boundary conditions for Ne and Ni impurities are scaled such that the Ne and Ni concentrations are consistent with charge-exchange recombination spectroscopy.

3. EDGE BACKGROUND PLASMA SOLUTIONS: SOLEDGE3X, SOLEDGE2D

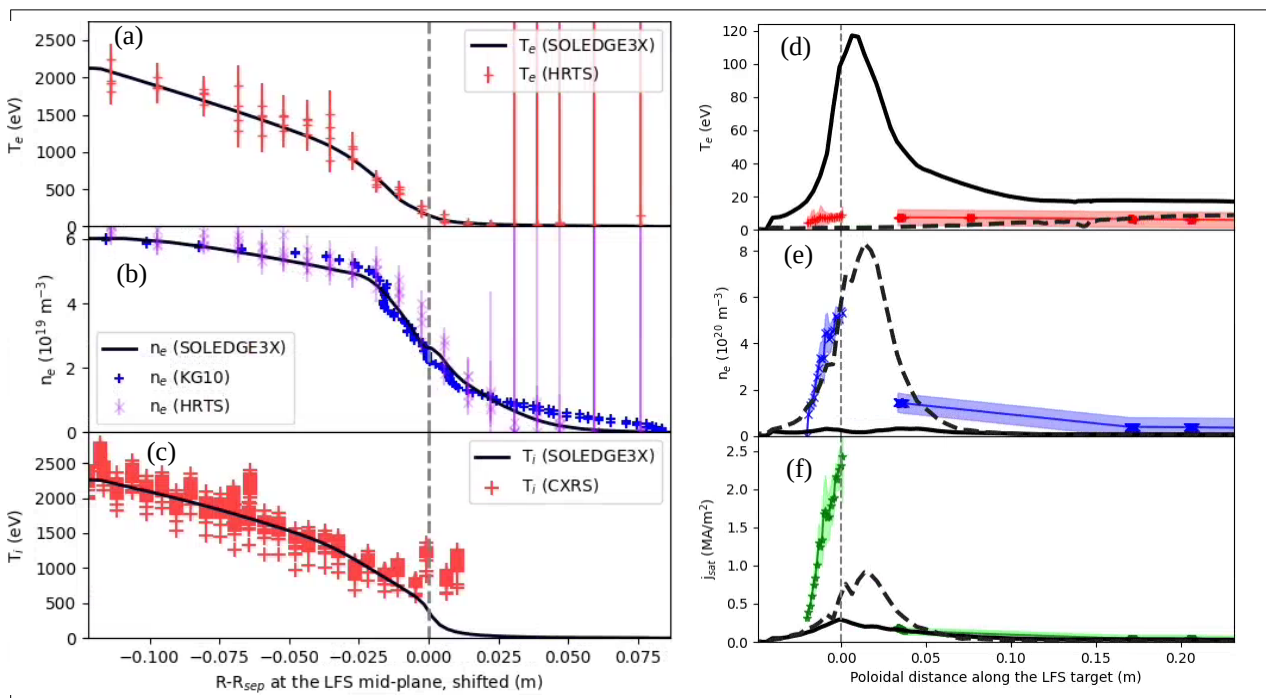


FIG. 2. Left: Simulated (SOLEDGE3X, black lines) and measured T_e (Thomson scattering (HRTS), (a)), n_e (reflectometry (KG10) and Thomson scattering, (b)), and T_i (charge-exchange recombination spectroscopy (CXRS), (c)) profiles along the LFS mid-plane, #97490 at 15 s. Right: Simulated (black lines) and measured (Langmuir probes, markers) T_e (d), n_e (e), and j_{sat} (f) profiles along the LFS target. Solid lines indicate SOLEDGE3X with drifts and dashed lines SOLEDGE2D without drifts.

For the purpose of modelling W transport into the main chamber, the SOLEDGE3X plasma solution with drifts is preferable over SOLEDGE2D without drifts for several reasons:

- (a) Simulations with drifts provide a solution for the plasma potential, used to calculate the parallel and radial electric fields needed by ERO2.0.
 - (b) Drifts significantly alter the main ion flow in the scrape-off layer (SOL), thereby also W screening.
- (c) Inclusion of the drifts results in a more complete description of the relevant physical processes, often found to improve code-experiment agreement on the density and temperature profiles, including inner-outer divertor asymmetries [15].

However, despite successful validation along the LFS mid-plane (Fig. 2a), the currently available SOLEDGE3X solution overestimates T_e and underestimates n_e and ion saturation current (j_{sat}) along the LFS divertor target (Fig. 2b). Hence, both the semi-detached SOLEDGE2D solution, which more closely describes the LFS divertor conditions, and the attached SOLEDGE3X solution are used to calculate a lower and upper estimate respectively of the W erosion rate at the LFS target. The charge-state resolved Ne flux incident on ERO2.0 wall surfaces is taken from SOLEDGE2D for both the drift and no-drift cases.

4. W EROSION SOURCES AND W I LINE EMISSION: ERO2.0

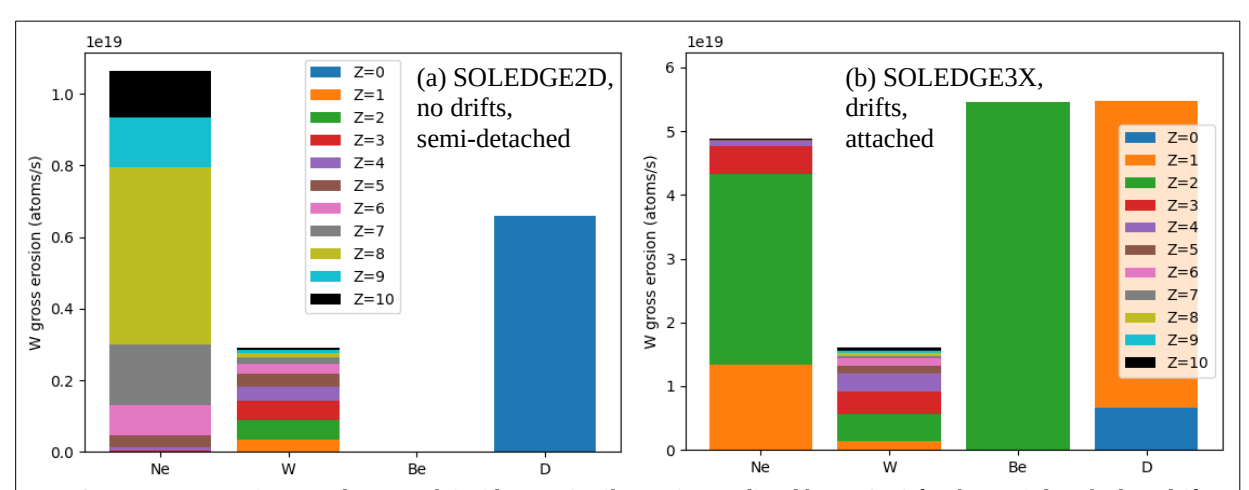


FIG. 3. W gross erosion rate due to each incident projectile species predicted by ERO2.0 for the semi-detached no-drift SOLEDGE2D solution (a) and for the attached SOLEDGE3X solution with drifts (b), as a sum over all W divertor components. A constant Be^{2+} concentration of 0.5% is imposed in both cases. Negligible self-sputtering contributions of W^{11+} and higher charge states are not shown.

ERO2.0 simulations based on the no-drift SOLEDGE2D solution predict Ne ions as the dominant cause of W erosion, followed by D atoms and W self-sputtering (Fig. 3a). Due to partial detachment at both divertor targets, Ne charge states Ne^{4+} and higher are required to reach impact energies with significant $Ne \rightarrow W$ sputtering. These Ne charge states are mostly prevalent in the far SOL, especially on the high-field side (HFS).

Most of the W erosion by D atoms occurs in the far SOL near the LFS divertor shoulder, because the CXN flux from the pedestal is attenuated by the denser plasma along the HFS and at the divertor targets. The flux of energetic CXN reaches another local maximum at the LFS main chamber wall, which is not made of W. Unlike D atoms, the contribution of Be and D ions to W sputtering is negligible at all plasma-facing components due to low impact energy.

When drifts are included in the background plasma solution, W erosion at the HFS divertor shoulder is suppressed by very low $T_e < 1$ eV, and the attached LFS target is the dominant source of W erosion. The high simulated T_e in the near-SOL causes significant sputtering of W by Be, D, and Ne ions (Fig. 3b). The incident Be is imposed as Be^{2+} in the simulation for computational performance, but part of the Be^{2+} and Ne flux is expected to ionise to higher charge states with higher sputtering yield if Be and Ne ions were included as traced impurity species in ERO2.0.

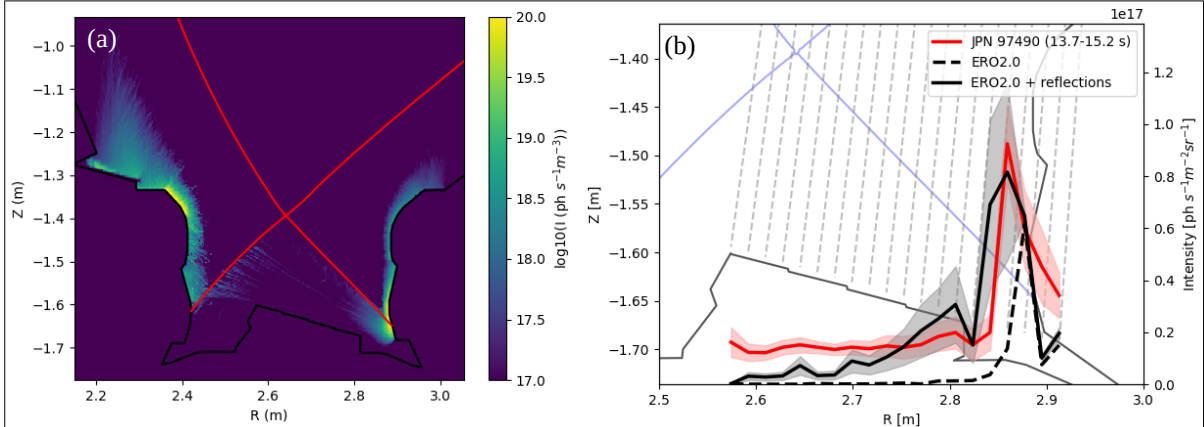
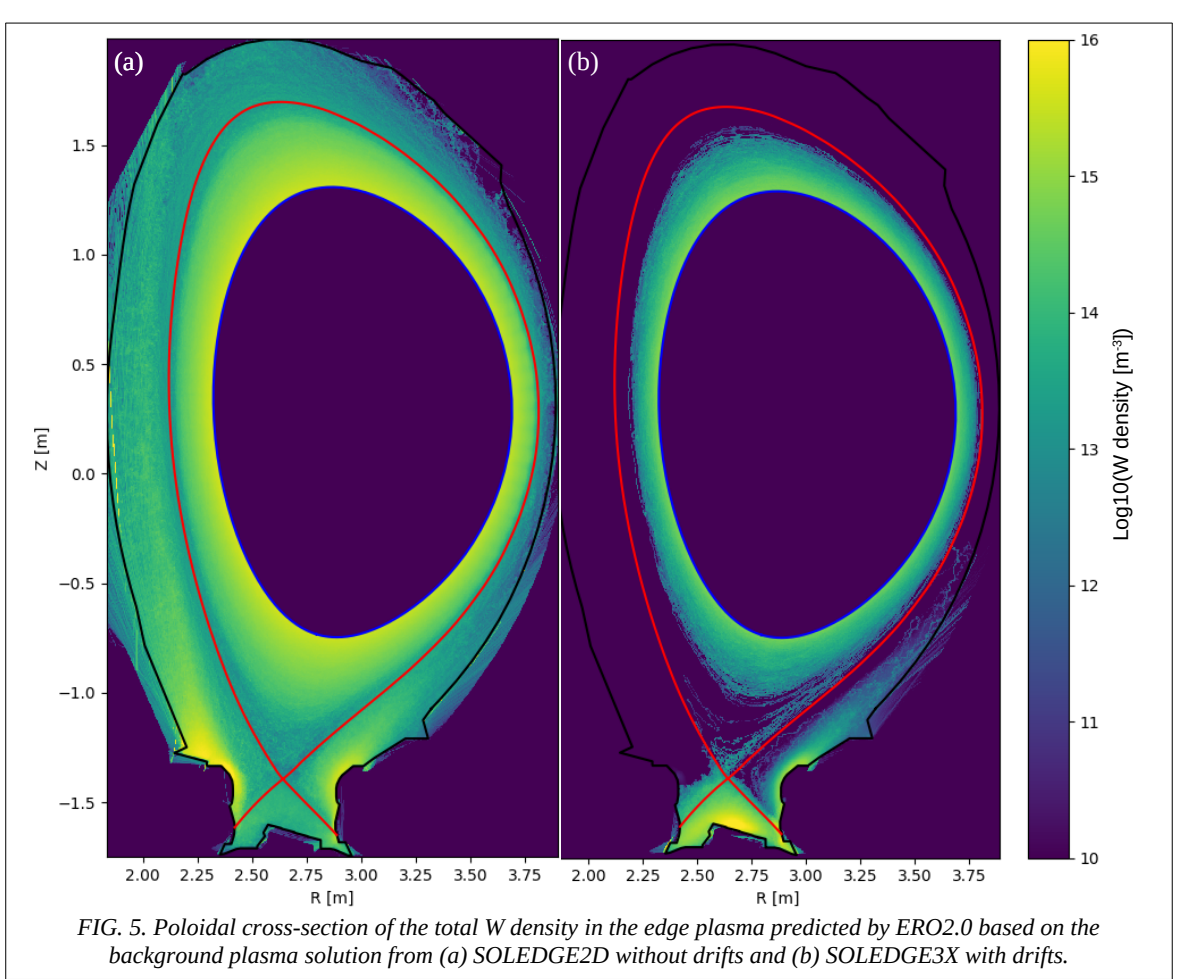


FIG. 4. (a) W I volumetric line emission intensity predicted by ERO2.0 in a 2D poloidal cross-section of the JET divertor. (b) Line-integrated W I emission profile measured by a spectrometer system (red) and synthetic W I measurements based on ERO2.0 (black) with and without photon reflections, #97490 at 13.7-15.2 s. The lines of sight are indicated in gray dashed lines.

H.A. KUMPULAINEN et al.

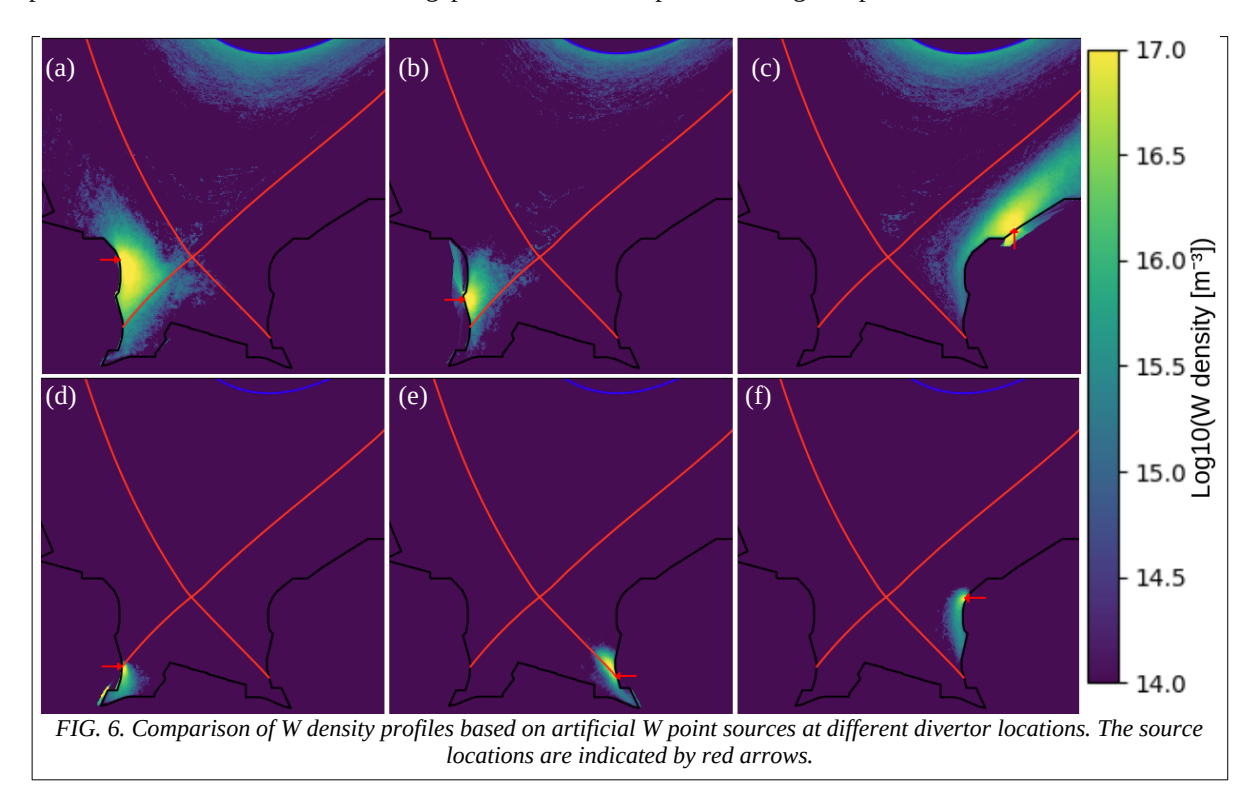
The volumetric W I line emission intensity profile predicted by ERO2.0 with the SOLEDGE2D no-drift plasma (Fig. 4a) is integrated along the spectrometer lines of sight to obtain a synthetic spectrometer measurement which is validated against measurements (Fig. 4b). The spectrometer view of the largest W erosion sources on the LFS is obstructed by the divertor shoulder, which is why most of the measured W I signal consists of photon reflections from the horizontal tiles at the bottom of the divertor. The ERO2.0 synthetic W I measurement based on volumetric W I emission only (Fig. 4b, dashed black line) matches the measurement at the divertor shoulder in direct view of the spectrometer, but the location of the emission peak is located radially further outward than in measurements. To account for surface reflections, Monte Carlo photon mapping of the volumetric photon source is applied in the post-processing phase to calculate the surface radiance at each wall location and the radiated intensity in the spectrometer viewing direction. Phong reflections [16] are assumed with a total reflectivity of 0.4 +/- 0.2 at the W surfaces (Fig. 4b, solid black line with confidence intervals). With photon reflections included, the synthetic W I signal predicted by ERO2.0 is more consistent with the measurement and matches the observed location of the emission peak. The significant differences between the measured and simulated Te, ne, and jsat at the target have a remarkably weak net impact on the W I emission, partly because fewer W I photons per eroded W atom are emitted at higher T_e. The total W I intensity predicted by ERO2.0 is comparable using the SOLEDGE2D and SOLEDGE3X plasma solutions, despite the different gross W erosion rates, mainly due to faster redeposition in the higher erosion case.

5. W EDGE TRANSPORT: ERO2.0



The ERO2.0 simulation case based on the SOLEDGE3X solution with drifts predicts a factor-of-10 lower W density in the core plasma than in the no-drift case, despite an order of magnitude higher gross W erosion rate (Fig. 5). The primary W source at the LFS divertor target has virtually no impact on the core plasma due to divertor screening driven by parallel-B SOL transport. Instead, the W density at the separatrix is determined mostly by W sources in the far SOL, above the divertor entrance, and by the balance of parallel-B

and radial transport in the main chamber SOL. The W density is non-zero in certain locations outside the poloidal wall contour due to toroidal gaps between the 3D plasma-facing components.



To further quantify the effectiveness of divertor screening at different locations, additional ERO2.0 simulations of the SOLEDGE3X drift case are carried out with artificial W point sources instead of W sputtering (Fig. 6). W sources at both the HFS and LFS strike lines are fully screened (Fig. 6d, 6e). HFS W sources in the far-SOL have a non-negligible probability of reaching the confined plasma via the X-point (Fig. 6a, 6b), with screening efficiency improving towards the strike line. W sources in the outer vertical divertor are efficiently screened (Fig. 6f), but W sources on top of the outer divertor shoulder have the weakest screening of the studied divertor locations. In all 6 cases, the resulting W density in the main plasma is less than 0.05% of what ERO2.0 predicts for a W source of the same magnitude at the outer mid-plane separatrix. The initial velocity of the injected W atoms is sampled from an isotropic Maxwellian distribution with T = 10 eV.

Compared to the no-drift case, drifts in the background plasma reduce the effectiveness of W screening on the HFS due to lower T_e , thus longer ionisation mean-free path, but improve W screening in the LFS far-SOL due to significantly higher n_e and T_e . The weaker W screening on the HFS does not result in excessive W influx because the predicted W erosion rate in the detached HFS far-SOL is negligible. In contrast, the improved W screening on the LFS greatly reduces the predicted W influx to the main chamber, resulting in the observed factor-of-10 difference in the main plasma W density (Fig. 5).

6. W CORE TRANSPORT: JINTRAC

The plasma profiles simulated in JETTO with optimised Bohm-gyro-Bohm transport multipliers closely agree with the measured n_e , T_e , and T_i profiles (Fig. 7). The best-fit multipliers are 0.68 for particle diffusion, 2.4

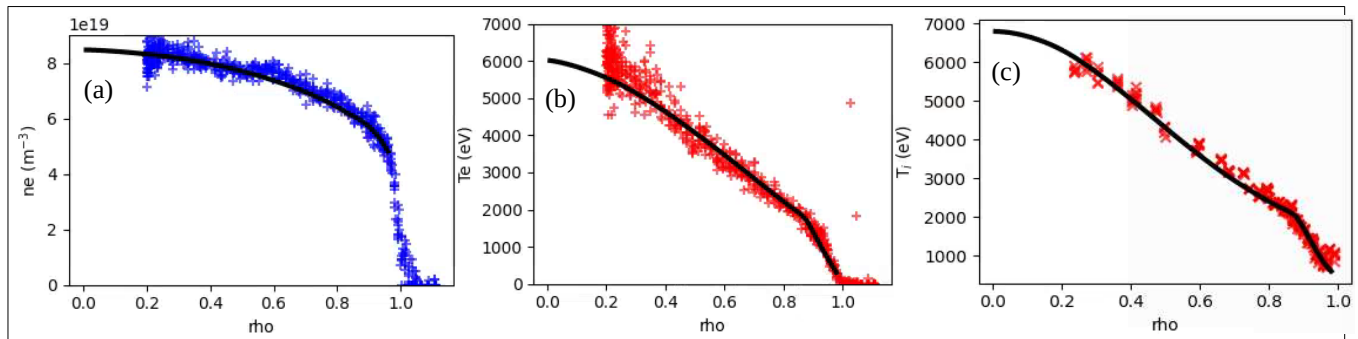


FIG. 7. Comparison of plasma profiles simulated using JETTO (black solid lines) with the measured (markers) (a) n_e (Thomson scattering), (b) T_e (Thomson scattering), and (c) T_e (CXRS) profiles as a function of the normalised minor radius ρ in #97490 at 15 s.

H.A. KUMPULAINEN et al.

for electron thermal and 3.3 for ion thermal diffusion. Additionally, a particle diffusion linear weight scaling from 2.0 in the core to 0.045 at the edge is applied to achieve the correct shape of the n_e profile. Accurate n_e and T_i gradients are critical due to their very strong impact on neoclassical W transport.

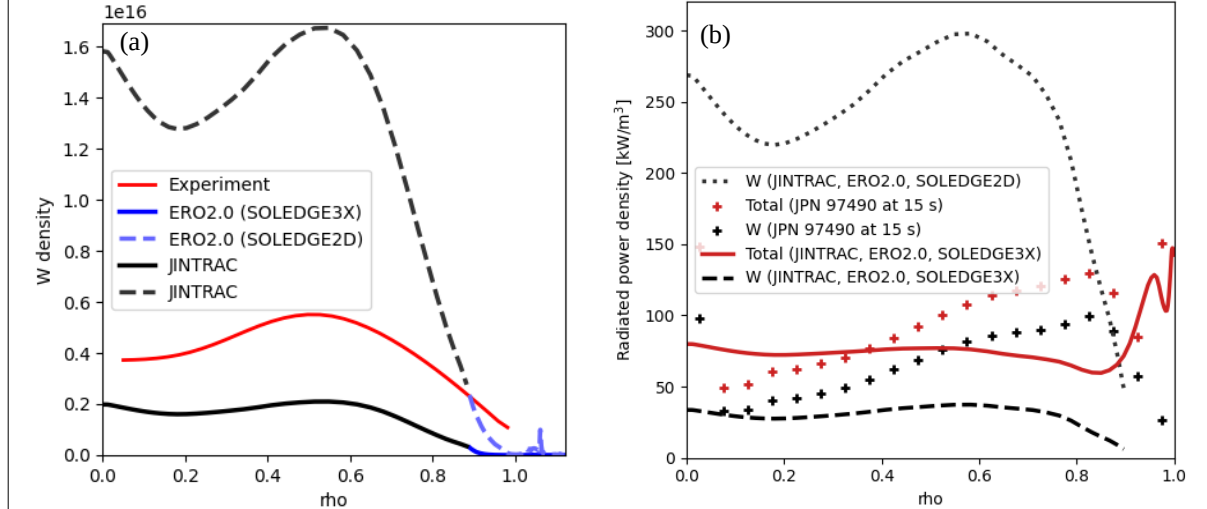


FIG. 8. (a) Flux-surface averaged W density profile based on an integrated data analysis [17] of measurements (red), predicted by ERO2.0 in the edge (blue), and predicted by JINTRAC in the core (black) with a boundary condition from ERO2.0 (black) in #97490 at 15 s. Dashed lines indicate SOLEDGE2D, solid lines SOLEDGE3X as edge background. (b) W (black) and total (red) radiated power density based on an integrated data analysis [17] of measurements (markers), and calculated based on JINTRAC (solid and dashed lines) with a boundary condition from ERO2.0.

The predicted W density and radiation profiles are validated by comparison against the experimentally inferred W density (Fig. 8a), W radiated power density, and total radiated power density profiles (Fig. 8b). When drifts are neglected, the predicted W radiation significantly exceeds the observed total radiation. Simulations with drifts yield a closer agreement with the experimental data than without drifts, although sizable uncertainties are associated with both the experimentally inferred and the predicted W density and radiation profiles.

7. CONCLUSIONS

The first application of the ERO2.0 + JINTRAC W erosion and transport workflow to JET Ne-seeded ELM-free H-mode demonstrates predicted W I line emission and core W density approximately within a factor of 3 of the measurements. The level of code-experiment agreement is within the significant modelling uncertainties (factor of > 3) stemming from diagnostic coverage, measurement accuracy, and the limited ability of background plasma simulations to replicate the measurements. The inclusion of photon reflections in synthetic diagnostics is found to be necessary to match the W I emission intensity and peak location, mainly due to obstructed spectrometer line-of-sight coverage of the primary W erosion source. Accounting for cross-field drifts in the edge background plasma modelling increases the predicted gross W erosion source, but reduces the W density in the main plasma by an order of magnitude compared to simulations without drifts.

Analysis of the experiments in conjunction with the ERO2.0 simulations reveals effective strategies for controlling W accumulation without requiring type-I ELMs. W screening is greatly improved by a wide high-density ionizing SOL that reduces the CX rate in the main plasma and attenuates the CXN flux, thereby reducing W erosion by atoms in the most weakly screened divertor locations. Additionally, the main ion parallel-B flow in the SOL provides excellent screening of W sputtered by Ne ions in the divertor, especially when the impact of drifts is considered. Increasing the magnitude of flows in the main chamber SOL and avoiding flow reversal in the near-SOL reduces the W density at the separatrix and consequently on all closed flux surfaces.

Unlike the JET hybrid scenario, which achieves W screening in the mantle region of the confined plasma via neoclassical ion temperature screening [18], the studied JET-ITER baseline scenario with a high-recycling LFS divertor has inward W convection across the mantle. Instead of outward convection, the JET-ITER baseline scenario achieves discharges with stationary radiation due to reduced W sources, a low n_e gradient in the

pedestal, and effective W screening in the SOL. Future studies on W erosion and transport in JET-ITER baseline plasmas include revised edge background plasma modelling to improve code-experiment agreement at the divertor targets.

ACKNOWLEDGEMENTS

This work is financially supported by a research grant awarded by the Finnish Cultural Foundation. The authors gratefully acknowledge computing time on the supercomputer JURECA at Forschungszentrum Jülich under Grant No. CJIEK43. This work has been carried out within the framework of the EUROfusion Consortium, funded by the European Union via the Euratom Research and Training Programme (Grant Agreement No 101052200 — EUROfusion). Views and opinions expressed are however those of the author(s) only and do not necessarily reflect those of the European Union or the European Commission. Neither the European Union nor the European Commission can be held responsible for them.

REFERENCES

- [1] KUMPULAINEN, H.A. et al., "Validated edge and core predictions of tungsten erosion and transport in JET ELMy H-mode plasmas", Plasma Phys. Control. Fusion **66** (2024) 055007.
- [2] KUMPULAINEN, H.A. et al., "Validation of EDGE2D-EIRENE and DIVIMP for W SOL transport in JET", Nucl. Mater. Energy **25** (2020) 100866.
- [3] GIROUD, C. et al., "The core–edge integrated neon-seeded scenario in deuterium–tritium at JET", Nucl. Fusion **64** (2024) 106062.
- [4] GIROUD, C. et al., "High performance ELM-free semi-detached scenario sustained at high-current in JET DTE3", this conference.
- [5] BUFFERAND, H. et al., "Progress in edge plasma turbulence modelling-hierarchy of models from 2D transport application to 3D fluid simulations in realistic tokamak geometry", Nucl. Fusion **61** (2021) 116052.
 - [6] REITER, D. et al., "The EIRENE and B2-EIRENE codes", Fusion Sci. Technol. 47 (2005) 172.
- [7] KUMPULAINEN, H.A. et al., "Impact of bivariate energy and angular atomic impact spectra on tungsten erosion in JET", Plasma Phys. Control. Fusion **67** (2025) 055044.
- [8] ROMAZANOV, J. et al., "Beryllium global erosion and deposition at JET-ILW simulated with ERO2.0", Nucl. Mater. Energy **18** (2019) 331–8.
- [9] BELLI, E.A., CANDY, J., "Kinetic calculation of neoclassical transport including self-consistent electron and impurity dynamics", Plasma Phys. Control. Fusion **50** (2008) 095010.
- [10] CENACCHI, G., TARONI, A., "Jetto a free boundary plasma transport code", Rapporto ENEA RT/TIB (88)5, Rome, Italy, 1988.
- [11] ROMANELLI, M. et al., "JINTRAC: a system of codes for integrated simulation of tokamak scenarios", Plasma Fusion Res. **9** (2014) 3403023.
- [12] HO, A. et al., "Neural network surrogate of QuaLiKiz using JET experimental data to populate training space", Phys. Plasmas **28** (2021) 032035.
- [13] ERBA, M., CHERUBINI, A., PARAIL, V.V., SPRINGMANN, E., TARONI, A., "Development of a non-local model for tokamak heat transport in L-mode, H-mode and transient regimes", Plasma Phys. Control. Fusion **39** (1997) 261.
- [14] HOULBERG, W.A., SHAING, K.C., HIRSHMAN, S.P., ZARNSTORFF, M.C., "Bootstrap current and neoclassical transport in tokamaks of arbitrary collisionality and aspect ratio", Phys. Plasmas **4** (1997) 3230.
- [15] BOEYAERT, D. , CARLI, S., DEKEYSER, W., WIESEN, S., BAELMANS, M., "Numerical implications of including drifts in SOLPS-ITER simulations of EAST", Phys. Plasmas **31** (2024) 023905.
 - [16] PHONG, B.T., "Illumination for computer generated pictures", CACM **18** 6 (1975) 311–317.
- [17] LITHERLAND-SMITH, E. et al., "High and medium Z impurity concentration determination with InDiCA in JET", 51st European Physical Society Conference on Plasma Physics (Vilnius, Lithuania, 2025), 4 P 296.
- [18] FIELD, A. et al., "Peripheral temperature gradient screening of high-Z impurities in optimised 'hybrid'scenario H-mode plasmas in JET-ILW", Nucl. Fusion **63** (2023) 016028.